

Cluster density slopes from Dark Matter-Baryons Energy Transfer

Antonino Del Popolo,^{1,2,*} Morgan Le Delliou,^{3,4,5} and Maksym Deliyergiyev⁶

¹*Dipartimento di Fisica e Astronomia, University Of Catania, Viale Andrea Doria 6, 95125, Catania, Italy*

²*Institute of Astronomy, Russian Academy of Sciences, 119017, Pyatnitskaya str., 48, Moscow*

³*Institute of Theoretical Physics, School of Physical Science and Technology, Lanzhou University, No.222, South Tianshui Road, Lanzhou, Gansu 730000, China*

⁴*Instituto de Astrofísica e Ciências do Espaço, Universidade de Lisboa, Faculdade de Ciências, Ed. C8, Campo Grande, 1769-016 Lisboa, Portugal[†]*

⁵*Lanzhou Center for Theoretical Physics, Key Laboratory of Theoretical Physics of Gansu Province, Lanzhou University, Lanzhou, Gansu 730000, China*

⁶*Département de Physique Nucléaire et Corpusculaire, University of Geneva, CH-1211 Geneve 4, Switzerland[‡]*

(Dated: August 18, 2021)

In this paper, we extend previous works on the relation between mass and the inner slope in dark matter density profiles. We calculate that relation in the mass range going from dwarf galaxies to cluster of galaxies. This was done thanks to a modeling of energy transfer via SN and AGN feedback, as well as via dynamical friction of baryon clumps. We show that, in the mass range above galaxy masses (Groups and clusters), the inner slope-mass relation changes its trend. It flattens (towards less cuspy profile) around masses corresponding to groups of galaxies and steepens again for large galaxy cluster masses. The flattening is produced by the AGN outflows (AGN feedback). The one- σ scatter on α is approximately constant in all the mass range ($\Delta\alpha \simeq 0.3$). This is the first paper extending the inner density profile slope-mass relationship to clusters of galaxies, accounting for the role of baryons. The result can be used to obtain a complete density profile, also taking baryons into account. Such kind of density profile was previously only available for galaxies.

Keywords: Dark matter; Galaxy clusters; Evolution of the Universe

I. INTRODUCTION

The content of the Universe is clearly not reduced to ordinary baryonic matter, as seen in the gravitational effects at the cosmological level [1], mixed with astrophysical scale effects [2, 3], where observations strongly point towards non-baryonic mass/energy domination of mass content by a clustering component coined dark matter (DM). Cosmological observations of the Universe's accelerated expansion [4, 5] further indicate overall domination by the component responsible for this acceleration called dark energy (DE).

The baryonic, DM and DE densities are measured to make up, respectively, 4.9%, 26.4% and 68.7% of our Universe.

Our most successful model for such universe, based on the big-bang cosmology, uses the cosmological constant Λ as DE and describes the rest with five further parameters. Designated as the Λ CDM (Cold DM with Λ) model, this paradigm, although it was very successful to explain many phenomena, as found in numerous studies including [3, 6–10], remains plagued with unexpected discrepancies compared with specific observations, as well as theoretical challenges: the deep theoretical challenges include what is known as the cosmological constant problems [11, 12], related also to the unknown natures of DE [13–15] and DM. From an observational perspective, anomalies accumulate at the large scales, in tensions of the Cosmic Microwave Background (CMB) Planck 2015

data with the Hubble parameter measured in type Ia Supernovae (SNIa, or simply SN) [16], with the CFHTLenS weak lensing [17], or with its σ_8 values [18]. At small scales, they are embodied within the so-called "small scale problems" [galactic, and centre of galaxy clusters scales, discussed, e.g., in 3, 19–25]. They comprise *a*) the anomalous gap between observations and N-body simulations predictions on the number of galactic subhaloes [e.g. 26]; *b*) the so-called Too-Big-To-Fail (TBTf) problem: simulated haloes produce too many, too massive and dense subhaloes, that cannot be disrupted to explain their absence in observations [27, 28].

Those two problems found a proposal for a unified solution, based on the effect of baryons within the haloes' inner parts [29, 30].

c) the Cusp/Core problem remains the most persistent of the Λ CDM paradigm problems [31, 32] and points at the inconsistency between LSBs and dwarf galaxies observed flat density profiles and the cuspy profiles produced in N-body simulations, e.g. the Navarro-Frenk-White (NFW) profile [33–35].

This paper will focus on the so-called Cusp/Core problem. The density profiles from simulations already are subjects of discussions, focussing on the slopes for the inner region of haloes: the NFW profile predicts an inner profile characterised by density $\rho \propto r^\alpha$, with $\alpha = -1$, [36] and [37] produced even steeper profiles, with $\alpha = -1.5$, while other works encounter object and/or even mass dependent inner slopes [38–46]. The Einasto profile, flattening towards the centre to $\alpha \simeq -0.8$ [47] seems to provide a better fit to simulations [48]. The claim of universal density profiles have been contradicted in [49], where their initial linear density perturbation power spectra determine their shape, which also depend on their mass. This mass dependence agrees with previous works and with pos-

* adelpopolo@oact.inaf.it

[†] Corresponding author: delliou@lzu.edu.cn Morgan.LeDelliou.ift@gmail.com

[‡] maksym.deliyergiyev@unige.ch

sible cores development in the warm DM (WDM) paradigm, however not significantly enough to explain observations.

In this debated context for the inner slope of haloes, the Cusp/Core problem resides in that dissipationless N-body simulations smallest predicted inner slopes exceed those obtained from SPH simulations [50, 51], semi-analytical models [52–56], or observations [57–62].

Although the Cusp/Core discussion started from galaxy scale haloes, it also has impact at galaxy clusters scales. Even though clusters total mass profiles agree with NFW predictions [22, 23, 63–65], lensing and kinematics constraints applied in relaxed clusters’ central cD galaxies (Brightest Central Galaxies, BCG) found flatter DM profiles than the NFW.

The simple dynamical structure (bulgeless disks) of dwarf galaxies and their DM domination with low baryon fraction [66] made them widely used in the Cusp/Core debate, as the determination of the inner density structure of larger, high surface brightness (HSB) objects is more complicated and the universality of galaxies’ cored nature is not definitely established: some authors claim HSBs are cored [67] when others differ [e.g., 21, 45, 68–70]. While low luminosity galaxies, $M_B > -19$, in the THINGS sample, tend to follow isothermal (ISO) profiles, cuspy or cored profiles describe equally well its galaxies with $M_B < -19$. The inner profile of dwarfs galaxies also varies [68]: among NGC 2976, 4605, 5949, 5693, and 6689, it ranges from 0 (NGC2976) to -1.28 (NGC5963). The confusion increases when noting that similar techniques on the same object yield different results: for, e.g., NGC2976, [71] obtained $-0.17 < \alpha < -0.01$ for the DM slope, while [72] got $\alpha = -0.90 \pm 0.15$, [73] traced $\alpha = -0.53 \pm 0.14$ with stars, or $\alpha = -0.30 \pm 0.18$ was derived using gas by [73].

This discussion reveals the difficulties associated with galaxies inner slope determination, including for dwarfs. It shows the existence of a range of slopes and the lack of agreement on their distribution despite recent kinematic maps [62, 68, 73].

The confusion increases further for smaller masses (e.g. dwarf spheroidals (dSphs)) and larger masses (e.g., spiral galaxies), where stars dominate¹, when biases enter models [74] and yields opposite outcomes.

Evaluation of central slopes of dSphs can employ different methods: as mass and stellar orbits anisotropy are degenerate in the spherical Jean’s equation model, its results strongly depend on the model’s assumptions [75]; a similar drawback also plaguing the maximum likelihood method applied to Jean’s model parameter space [76–78]. Schwarzschild modelling found cored profiles for the Fornax and Sculptor profiles [79–82], in agreement with multiple stellar populations methods that can measure central slopes at $\simeq 1$ kpc (Fornax) and even $\simeq 500$ pc (Sculptor) [83–86]. However the Schwarzschild model applied to Draco found a cusp [82]. In general, there is not consensus on the inner structure of dSphs. A recent paper [87] found different, and cuspiers, halo density

profiles than previous estimates. Similarly, [88] showed that for Fornax, considered for a long time to harbour a 1 kpc core, a cuspy dark matter halo is probably not excluded.

Although dSphs can thus either be cored or cusped, their DM dominated dynamics should yield cuspy central profiles, at least for smaller masses.

Given observations, two kinds of approaches could solve the Cusp/Core problem:

- 1) cosmological solutions, comprising
 - (a) modified small scale initial spectrum [e.g. 89],
 - (b) various DM particles nature [90–95],
 - (c) modified gravity theories, e.g., $f(R)$ [96, 97], $f(T)$ [see 98–101] or MOND [102, 103].
- 2) Astrophysical solutions, that reduce galaxies’ inner density from DM component expansion induced by some ”heating” mechanism, such as
 - (a) ”supernovae feedback“ cusp flattening (SNF) [50, 51, 104–111],
 - (b) ”dynamical friction from baryonic clumps” (DFBC) [52, 112–120].

We will concentrate here in the astrophysical solutions 2), and in particular in the DFBC 2)b, discussed further in the following sections.

The SNF model has been studied in a large number of papers, and has been shown to be most effective for galaxies smaller than the Milky Way [50, 51, 104, 121–123].

Although successful in some cases, the SNF model is less so in others. Its effects depend, among other things, on the nature of star formation. For instance, for the SNF, cosmological simulations with lower density thresholds for star formation, e.g. APOSTLE and Auriga [124], do not produce DM cores. Furthermore, the THINGS galaxies [69, 125] density profiles [61, 62, 126] agreed with the [50] SNF model, while simulations of both disk galaxies and dwarfs from [127], including the SNF model along with feedback from massive stars radiation pressure, found radiation pressure to dominate SNF effects in core formation, so SNF alone cannot form cores. In general, the SNF as possible solution to Λ CDM small scale problems has been questioned in many works [128–132]. Core formation is also influenced by the ratio of DM halo growth time to star formation time. Mergers happening after core formation can rejuvenate a cusp [133].

Other papers, such as [134], claim an agreement between galaxies characteristics and simulations. [134] tested the prediction of [46] that claims core formation when the M_*/M_{halo} ratio between the stellar and halo masses is of the order or smaller than 0.01, while at larger values, SNF leads DM to expand, again tending to give rise to a core. The flattest profile forms when $M_*/M_{\text{halo}} \simeq 5 \times 10^{-3}$. For larger ratios, the structure’s central stellar component deepens the gravitational potential, opposing the SNF driven expansion, resulting in a cuspiers profiles. [122], using the FIRE-1 suite, and [123], by means of the NIHAO suite, confirmed the [46] result.

¹ See Section V for a wider discussion.

The work of [123] was extended by [135] to include black hole (BH) feedback, determining the mass-slope relation over eight orders in magnitudes in stellar mass. [136] compared the ability of the SNF and the DFBC mechanisms to solve the Cusp/Core problem through their theoretical predictions vs observations of the inner slopes of galaxies confrontation, with masses ranging from dSphs to normal spirals. It found both mechanisms to give similar results. The DFBC achievements, summarised hereafter, are also described in Sec. II. It predicted the correct shape of galaxy density profiles [52, 137] in agreement with [50, 51] SPH simulations. Similarly in the case of clusters, the density profile in [54] matches predictions from the profiles simulated by [138]. Furthermore, several galaxy clusters predictions from [54] are in agreement with the observations in [22, 23]. The work in [42] had already found the dependence of the inner slope on mass claimed later by [46]. Such slope-mass dependence had been reported over masses ranging from dwarf galaxies to clusters [3, 42, 52, 54, 55]. The DFBC model found a series of additional correlations such as between

- a) inner slope and 1) the baryon to halo mass ratio M_b/M_{500}^2
- 2) angular momentum³ as seen in [55], while, in agreement with [22, 23], the inner slope also correlates with 3) the Brightest Cluster Galaxy (BCG) mass, 4) the core radius r_{core} , 5) the effective radius R_e , and
- b) between the DM dominated mass inside 100 kpc, and the mainly baryonic [140] mass inside 5 kpc.

Ref. [123] confirmed the results of [46], and extended it to redshift $z = 1$. The FIRE-2 galaxy formation physics simulated 54 galaxy halos, which CDM density profiles were analyzed in [141]. Ref. [135] added 46 new high resolution simulations of massive galaxies, including BH feedback, to the work of [123]. This allowed to trace the DM halo inner slope dependence from galaxies to groups of galaxies.

In this context, [42] showed the halo density profiles inner slope of spiral galaxies depend on their mass. That result was extended in [136] to spheroidal galaxies. For dSphs with baryonic mass smaller than $10^9 M_\odot$, the DM halo density profile was shown to steepen towards smaller masses. The slope shows a maximum flattening at $\simeq 10^9 M_\odot$, before steepening again for larger masses. A similar dependence was reported by [46], which work was extended by [123, 135, 141]. The NIHAO and FIRE results were compared in [87, Fig. 6] for the slope-mass relation [also see 141, Fig. 2]. The [141] slope-mass relation exclusively concerned galaxies, while only [135] extended it to groups of galaxies. In this paper, we aim to extend that study to galaxy clusters, including AGN feedback effects. That purpose will lead us to improve and extend the [136] model, using the [25] model for AGN feedback. Building a dwarf galaxies-cluster size halo mass range, including DM and baryonic effects, will enable for the first time the construction of a mass-dependent DM

density profile set. Recall that the [46] profiles only concerned galaxies.

This paper aims to extend some of the results of [136], namely those related to the slope-mass relationship. Ref. [136], among other results, showed how the slope of the inner DM density profile depends on baryonic and halo mass.

The mass range studied went from dwarf galaxies to galaxies similar to our Galaxy. The present paper extends that range to clusters of galaxy masses. To date, halo density profile taking baryons into account are only available for galaxies with mass similar to the Milky Way's.

The importance of the present results lies in the possibility it opens to compare the observed slopes of dwarf, and ultra faint galaxies, and thus discriminate which mechanism gives rise to the inner structure of those galaxies. Indeed, the slope of our model shows a maximum flattening at stellar masses $\simeq 10^8 M_\odot$. At smaller masses the steepening reaches a value of $\alpha \simeq -0.6$ at $M_{\text{star}} \simeq 10^4 M_\odot$. Such steepening at small masses is smaller than in the case of models based on supernovae feedback, such as [46, 123]. In other words, the model predicts that dwarf galaxies are less cuspy than predicted by [46, 123]. Consequently, dwarf, or ultra-faint galaxies with an almost cored profile means that the DFBC mechanism is the responsible of the core formation, while a cuspy profile implies that supernovae feedback has the main role in the cusp formation.

The paper is organized as follows. In Sec. II we describe the model that we will use, which implementation is summarised in Sec. III. Sec. IV discusses SNF and the DFBC mechanisms. Secs. V and VI are devoted to results and conclusions, respectively.

II. THEORETICAL MODEL

This section recalls the model employed in this work. The spherical collapse models [142–147] was very significant improved in [e.g. 52, 137] to include the effects of

- random angular momentum induced by random motion during the collapse phase of haloes [e.g., 145, 147],
- ordered angular momentum induced by tidal torques [e.g., 19, 148, 149],

and was furthered to include the consequences of

- adiabatic contraction [e.g., 150–153],
- dynamical friction between DM and baryonic gas and stellar clumps [52, 112–114, 116–120],
- gas cooling, star formation, photoionization, supernova, and AGN feedback [138, 154, 155] and
- DE [13–15],

and was further refined in [56, 136, 156, 157]. This model produced results on

- the universality of density profiles [42, 44],
- specific features of density profiles in
 - galaxies [3, 54] and
 - clusters [3, 55],

as well as a focus on

- galaxies inner surface-density [45].

² Recall R_{500} encloses 500 times the critical density and a mass M_{500} .

³ Larger mass structure collapse is reduced since their acquired angular momentum follows the peak height in inverse proportion [52, 139].

Although the model’s key mechanism resides in dynamical friction (DFBC), we stress out that it includes all of the above effects (including SNF) that each only contribute at the level of some %.

Its implementation occurs in several stages:

1. The diffuse proto-structure of gas and DM expands, in the linear phase, to a maximum radius before DM re-collapses into a potential well, where baryons will fall.
2. In their radiative clumping, baryons form stars at the halo centre.
3. Then four effects happen in parallel
 - (a) the DM central cusp increases from baryons adiabatic contraction (at $z \simeq 5$ in the case of $10^9 M_\odot$ galaxies [52])
 - (b) the galactic centre also receive clumps that collapse from baryons-DM dynamical friction (DF)
 - (c) the DF energy and angular momentum (AM) transfer to DM [and stars 106, 121, 158] results in an opposite effect to adiabatic contraction, and reduces the halo central density [112, 113].
 - (d) the balance between adiabatic contraction and DF can result in heating cusps and forming cores, i.e. in dwarf spheroidals and spirals, while the deeper potential wells of giant galaxies keeps their profile steeper.
4. The effect of DF adds to that of tidal torques (ordered AM), and random AM.
5. Finally, the core further slightly (few percent) enlarges from the decrease of stellar density due to successive gas expulsion from supernovae explosions, and from the disruption of the smallest gas clumps, once they have partially converted to stars [see 120].

II.1. Model treatment of density profile

Starting from a Hubble expansion, the spherical model of density perturbations expands linearly until reaching a turnaround maximum and reverting into collapse [159, 160]. A Lagrange particle approach yields the final density profile

$$\rho(x) = \frac{\rho_{\text{ta}}(x_m)}{f(x_i)^3} \left[1 + \frac{d \ln f(x_i)}{d \ln g(x_i)} \right]^{-1}, \quad (1)$$

with initial and turn-around radius, resp. x_i and $x_m(x_i)$, collapse factor $f(x_i) = x/x_m(x_i)$, and turnaround density $\rho_{\text{ta}}(x_m)$. The turn-around radius is obtained with

$$x_m = g(x_i) = x_i \frac{1 + \bar{\delta}_i}{\bar{\delta}_i - (\Omega_i^{-1} - 1)}, \quad (2)$$

where we used Ω_i for the density parameter, and $\bar{\delta}_i$ for the average overdensity inside a DM and baryons shell.

The model starts with all baryons in gas form with $f_b = 0.17 \pm 0.01$ for the ”universal baryon fraction“ [161] [set to 0.167 in 7], before star formation proceeds as described below.

Tidal torque theory (TTT) allows to compute the ”specific ordered angular momentum“, h , exerted on smaller scales from larger scales tidal torques [148, 162–165], while the ”random angular momentum“, j , is related to orbits eccentricity $e = \left(\frac{r_{\text{min}}}{r_{\text{max}}} \right)$ [166], obtained from the apocentric radius r_{max} , the pericentric radius r_{min} and corrected from the system’s dynamical state effects advocated by [146], using the spherically averaged turnaround radius $r_{\text{ta}} = x_m(x_i)$ and the maximum radius of the halo $r_{\text{max}} < 0.1 r_{\text{ta}}$

$$e(r_{\text{max}}) \simeq 0.8 \left(\frac{r_{\text{max}}}{r_{\text{ta}}} \right)^{0.1}. \quad (3)$$

These corrections to the density profile are compounded also with its steepening from the adiabatic compression following [151] and the effect of DF introduced in the equation of motion by a DF force [see 52, Eq. A14].

II.2. Effects of baryons, discs, and clumps

The baryon gas halo settles into a stable, rotationally supported, disk, in the case of spiral galaxies. Their size and mass result from solving the equation of motion, and lead to a solution of the angular momentum catastrophe (AMC) [Section 3.2, Fig. 3, and 4 of 3], obtaining realistic disc size and mass.

Notwithstanding stabilization from the shear force, Jean’s criterion shows the appearance of instability for denser discs. The condition for this appearance and subsequent clump formation was found by Toomre [167], involving the 1-D velocity dispersion σ ,⁴ angular velocity Ω , surface density Σ , related to the adiabatic sound speed c_s , and the epicyclic frequency κ

$$Q \simeq \sigma \Omega / (\pi G \Sigma) = \frac{c_s \kappa}{\pi G \Sigma} < 1. \quad (4)$$

The solution to the perturbation dispersion relation $d\omega^2/dk = 0$ for $Q < 1$ yields the fastest growing mode $k_{\text{inst}} = \frac{\pi G \Sigma}{c_s^2}$ (see [168] or [120, Eq. 6]). That condition allows to compute the clumps radii in galaxies [169]

$$R \simeq 7 G \Sigma / \Omega^2 \simeq 1 \text{ kpc}. \quad (5)$$

Marginally unstable discs ($Q \simeq 1$) with maximal velocity dispersion have a total mass three times larger than that of the cold disc, and form clumps $\simeq 10\%$ of their disk mass M_d [170].

Objects of masses few times $10^{10} M_\odot$, found in $5 \times 10^{11} M_\odot$ haloes at $z \simeq 2$, are in a marginally unstable phase for $\simeq 1$ Gyr. Generally the main properties of clumps are similar to those found by [171].

⁴ $\simeq 20 - 80$ km/s in most clump hosting galaxies

In agreement with [52, 114–120, 172], energy and AM transfer from clumps to DM flatten the profile more efficiently in smaller haloes.

II.2.1. Computing the clumps life-time

Evidence for existence of the clumps produced by the model can be traced both in simulations [e.g., 173–179], and observations. High redshift galaxies have been found to contain clump clusters or clumpy structures that leads to call them chain galaxies [e.g., 180–182]. The HST Ultra Deep Field encompasses galaxies with massive star-forming clumps [183, 184], many at $z = 1 - 3$ [185], some in deeper fields $z \lesssim 6$ [186].

Such clumpy structures are expected to originate from self-gravity instability in very gas-rich disc, from radiative cooling in the accreting dense gas [e.g., 171, 173, 187–189]. Their effect on halo central density depend crucially on the clump lifetime: should their disruption through stellar feedback still allow them sufficient time to sink to the galaxy centre, they can turn a cusp into a core. A clump’s ability to form a bound stellar system is assessed through its stellar feedback mass fraction loss, e_f , and its formed stars mass fraction, $\varepsilon = 1 - e_f$. Simulations and analytical models agree that most of the mass of such group of stars will remain bound for $\varepsilon \geq 0.5$ [190]. The radiation feedback efficiency can be estimated, using *a*) the dimensionless star-formation rate efficiency $\epsilon_{eff} = \frac{M_*}{M/t_{ff}}$. This is simply the ratio between free-fall time, t_{ff} , and the depletion time for a stellar mass M_* . In its reduced version it reads $\epsilon_{eff,-2} = \epsilon_{eff}/0.01$, *b*) the reduced dimensionless surface density $\Sigma_1 = \frac{\Sigma}{0.1g/cm^2}$, and *c*) the dimensionless reduced mass $M_9 = M/10^9 M_\odot$,

to obtain the expulsion fraction $e_f = 1 - \varepsilon = 0.086(\Sigma_1 M_9)^{-1/4} \epsilon_{eff,-2}$ [169]. Ref. [191] estimated, for a large sample of environments, densities, size and scales, that $\epsilon_{eff} \simeq 0.01$. Furthermore, $e_f = 0.15$ and $\varepsilon = 0.85$ for typical clumps with masses $M \simeq 10^9 M_\odot$. Therefore, the clump mass loss before they reach the centre of the galactic halo should be small. However, such conclusion and the expulsion fraction method are valid for smaller, more compact clumps in smaller galaxies. Such context only produces clumps that survive all the way to the centre.

Alternately, comparing a clump lifetime to its migration time to the centre, one can also obtain clump disruption. Migration time is the result of DF and TTT: for a $10^9 M_\odot$ clump, it yields $\simeq 200$ Myrs [see Eq. 1 of 120, 182, Eq. 18]. Coincidents expansion and migration timescales were computed from the Sedov-Taylor solution [182, Eqs. 8,9].

Clump lifetime has been much studied. Ceverino *et al.*, finding clumps in Jean’s equilibrium and rotational support, from hydrodynamical simulations [173], construed their long lifetime ($\simeq 2 \times 10^8$ Myr). This agrees with several approaches: in local systems forming stars and coinciding with the Kennicutt-Schmidt law, [169] found such lifetimes. This is because as clumps retained gas, and formed bound star groups, they had time to migrate to the galactic cen-

tre. Simulations from [192] confirmed it. Other simulations with proper account of stellar feedback, e.g. non-thermal and radiative feedback mechanisms, also obtained long-lived clumps reaching galactic centre [SNF, radiation pressure, etc 175, 176, 178]. Finally, the same was obtained with any reasonable amount of feedback [174]. The expansion, gas expulsion, and metal enrichment, time scales (respectively > 100 Myrs, 170-1600 Myrs, and $\simeq 200$ Myrs) obtained by [182] to estimate clump ages also bring strong evidence for long-lived clumps. Lastly, comparison between similar low and high redshift clumps observations [in radius, mass, 193–195] supports clump stability.

II.3. Model treatment of feedback and star formation

Star formation, reionisation, gas cooling, and SNF in the model are built along [154, 155, Secs. 2.2.2 and 2.2.3].

Reionisation acts for $z = 11.5 - 15$ by decreasing the baryon fraction as

$$f_{b,halo}(z, M_{vir}) = \frac{f_b}{[1 + 0.26M_F(z)/M_{vir}]^3}, \quad (6)$$

[155], using the virial mass, M_{vir} , and the “filtering mass” [see 196], M_F .

Gas cooling follows from a cooling flow model [e.g., 155, 197, see Sect. 2.2.2].

Star formation arises from gas conversion into stars when it has settled in a disk. The gas mass conversion into stars during a given time interval Δt , which we take as the disc dynamical time t_{dyn} , is given by

$$\Delta M_* = \psi \Delta t, \quad (7)$$

where the star formation rate ψ comes from the gas mass above the density threshold $n > 9.3/cm^3$ [fixed as in 46] according to [see 154, for more details]

$$\psi = 0.03 M_{sf}/t_{dyn}. \quad (8)$$

SNF follows [198], where SN explosions inject energy in the system. This energy can be calculated from a Chabrier IMF [199], using

- the disc gas reheating energy efficiency ϵ_{halo} ,
- the available star mass ΔM_* ,
- that mass conversion into SN measured with the SN number per solar mass as $\eta_{SN} = 8 \times 10^{-3}/M_\odot$, and
- the typical energy an SN explosion releases $E_{SN} = 10^{51}$ erg,

to obtain

$$\Delta E_{SN} = 0.5 \epsilon_{halo} \Delta M_* \eta_{SN} E_{SN}. \quad (9)$$

This released energy from SNs into the hot halo gas in the form of reheated disk gas then compares with the reheating energy ΔE_{hot} which that same amount of gas

should acquire if its injection in the halo should keep its specific energy constant, that is if the new gas would remain at equilibrium with the halo hot gas. That amount of disk gas the SN and stars radiation have reheated, ΔM_{reheat} , since it is produced from stars radiations, is proportional to their mass

$$\Delta M_{\text{reheat}} = 3.5 \Delta M_*. \quad (10)$$

Since the halo hot gas specific energy corresponds to the Virial equilibrium specific kinetic energy $\frac{V_{\text{vir}}^2}{2}$, keeping this energy constant under addition of that reheated gas leads to define the equilibrium reheating energy as

$$\Delta E_{\text{hot}} = 0.5 \Delta M_{\text{reheat}} V_{\text{vir}}^2. \quad (11)$$

The comparison with the actual energy of the gas injected from the disk into the halo by SNs gives the threshold ($\Delta E_{\text{SN}} > \Delta E_{\text{hot}}$) beyond which gas is expelled, the available energy to expel the reheated gas, and thus the amount of gas ejected from that extra energy

$$\Delta M_{\text{eject}} = \frac{\Delta E_{\text{SN}} - \Delta E_{\text{hot}}}{0.5 V_{\text{vir}}^2}. \quad (12)$$

Contrary to SNF based models such as [46], our mechanism for cusp flattening initiates before the star formation epoch. Since it uses a gravitational energy source, it is thus less limited in available time and energy. Only after DF shapes the core can Stellar and SN feedback occurs, which then disrupt gas clouds in the core [similarly to 120].

AGN feedback occurs when a central Super-Massive-Black-Hole (SMBH) is formed. We follow the prescriptions of [138, 200], modifying the [201] model for SMBH mass accretion and AGN feedback: a seed $10^5 M_{\odot}$ SMBH forms when stellar density, reduced gas density ($\rho_{\text{gas}}/10$) and 3D velocity dispersion exceed the thresholds $2.4 \times 10^6 M_{\odot}/\text{kpc}^3$ and 100 km/s , which then accretes. Significant AGN quenching starts above $M \simeq 6 \times 10^{11} M_{\odot}$ [202].

II.4. Model robustness

We point out that the model demonstrated its robustness in various behaviours:

- α . the cusp flattening from DM heating by collapsing baryonic clumps predicted for galaxies and clusters is in agreement with following studies [112, 113, 116–120]. A comparison with [50]’s SPH simulations was made in [44, Fig. 4].
- β . it aforesaid predicted the correct shape of galaxies density profiles [52, 137], ahead of SPH simulations of

[50, 51], and of clusters density profiles [55] anteriorly of [203].⁵

- γ . it aforesaid predicted the halo mass dependence of cusps inner slope [42, Fig. 2a solid line] beforehand the similar result in the non-extrapolated part of the plot in [46, Fig. 6], expressed in terms of V_c , as it corresponds to $2.8 \times 10^{-2} M_{\text{vir}}^{0.316}$ [204].
- δ . it also preceded [46] in predicting [see 55] that the inner slope depends on the total baryonic content to total mass ratio.
- ϵ . Fig. 6 in [46] compares well with the inner slope change with mass of [156, Fig. 2].
- ζ . it moreover provides a comparison of the Tully-Fisher and Faber-Jackson, $M_{\text{Star}} - M_{\text{halo}}$, relationships with simulations [156, Figs. 4, 5].

III. SUMMARY OF THE STEPS OF THE SIMULATION

Our model follows a semi-analytic approach, which is inexpensive compared with N-body/hydrodynamical simulations (such as NIHAO). This simplifies the construction of samples of galaxies, and rapid exploration of parameter space. Comparison studies of semi-analytic and N-body/hydro simulations have shown a good agreement in the studied cases [see 205, and references therein]. We use cosmological parameters as given by [135, Section 2]. Initially, the system is in gas form with the “universal baryon fraction” [161] $f_b = 0.17 \pm 0.01$ [set to 0.167 in 7]. The way initial conditions, starting from the power spectrum, are fixed, and their ensuing evolution, is described in [52, Appendix B]. When the system reaches the non-linear regime, tidal interaction with neighbors are calculated as shown in detail in [52, Appendix C]. In the collapse phase, random angular momentum is generated and is calculated as in [52, Appendix C]. The effect of dynamical friction is calculated in [52, Appendix D], while [52, Appendix E] shows how the baryonic dissipative collapse happens. In the collapse the system can give either rise to a spiral structure or to a spheroid. This is described in [136, Section A.5]. Clumps characteristics and formation are described in Section II. 2 of this paper. Stars form according to the scheme described in Section II. 3 of this paper. The black hole formation, and the AGN feedback are described in the final part of Section II. 3 of this paper. The NIHAO simulation is a hydrodynamical simulation, based on GASOLINE2: as reported in [135] it includes a series of physical effects like compton cooling, photoionisation and heating from the ultraviolet background, metal cooling, chemical enrichment, star formation and feedback from supernovae and massive stars.

⁵ Note that [50, 51] and [203] adopted different dominant mechanisms.

IV. DFBC AND SNF

This paper presents DFBC and SNF results within the model of Sec. II. In particular, it focusses on DM halo inner slopes. It will not quantitatively compare those with results from [135], as 1. such comparison was already presented in [136] for galaxies, using a large sample of data, against the [46] model, that displays results similar to [135]. 2. the [135] model only extends to the mass range of groups, while clusters of galaxies inner slope estimates are available [see 22, 23].

The role and importance of baryons in the Cusp/Core problem solution was suggested by Flores and Primack [32], and by several subsequent papers. [104] showed that the expulsion of gas in the halo in a single event could flatten the cusp. However, it was soon clear that a single event was not sufficient to produce observed flattening, and that repeated events were needed [206]. [107, 108], showed that random bulk motions of gas due to SN explosion could form a core. Governato [50, 51] confirmed the result, in addition to finding a correlation between stellar mass, M_* , and the inner slope for galaxies with $M_* > 10^6 M_\odot$. Their simulations, similarly to [46], implement SN feedback through early stellar feedback or the SN feedback. In fact, the inner slope characteristics dependence on stellar mass to halo mass ratio, M_*/M_{halo} , had already been found by [42].

An alternative mechanism to flatten cusps into cores was proposed by El-Zant [112, 113]. The model is based on "heating" of DM via interaction of baryons (gas clumps) with it through dynamical friction. The exchange of energy and angular momentum between clumps and dark matter can flatten the profile. The earlier the process occurs (i.e. for smaller halos), the more efficient it is. Many studies have confirmed the effectiveness of the process [3, 52, 114–118, 120]. In more detail, as shown by [3, 52], the DM and gas proto-structure starts in the linear phase. It expands to reach a maximum radius, and then recollapse. The collapse of the DM component occurs first, forming the potential wells in which baryons will fall. Because of radiative processes, baryons form clump, which collapse to the halo centre and form stars. The collapse also comprises the so called "adiabatic contraction" phase [150, 151], in which baryons are compressed, generating a cuspiest DM profiles.

Because of dynamical friction between DM and baryons, clumps fall to the centre of the structure. During this fall, angular momentum and energy is transferred to the DM component, and the cusp is heated, giving rise to the formation of a core. This core formation occurs before stars formation. Then, stellar feedback expels a large part of the gas, leaving a lower stellar density. After a part of the clumps is transformed into stars, feedback destroys clumps, and mass distribution is dominated by DM. The model just described agrees with [3, 52, 112, 114–118, 120].

This model is the only one able to describe the correct dependence of the inner slope of the DM density profile from dwarf galaxies to clusters of galaxies [42, 52, 54–56]. Apart from this, as described in the Sec. II, the model predicted several results, later also obtained by the SNF model.

The SNF and DFBC model differ significantly in the series

of steps they require. The SNF model starts from gas that forms stars. These can explode into supernovae if they have enough mass. A longer and more complex series of events are needed to produce the observed density profile flattening than for the DFBC. Indeed, the DFBC only requires the presence of gas clumps to flatten the halo cusp and gives rise to the core. DFBC is therefore more ergonomic and efficient at producing cores than the SNF model.

V. RESULTS

We used the model in Sect. II to determine the structure of the objects formed by DM and baryons. The density profile of every object was fitted to obtain the dependence of the inner slope on stellar and DM mass. The fitting method used is similar to that of [135]. After determining its center, the halo is divided in fifty spherical shells, each one with constant width in logarithmic scale. The halo density profile is obtained by evaluating, for each shell, the average DM density. The density profile central slope was then obtained, considering the shells with radius in the range 1%-2% of the virial radius⁶. The density profile central slope α was then computed with a linear fit in the $\log r - \log \rho$ plane.

The main results of the paper are plotted in Figs. 1-2, showing the relations between the inner density slope α , and the halo mass, or stellar mass, respectively. In both plots, the top solid lines represent the result of this paper, while the bottom ones that of [135]. Note that the dotted line in the [135] result is an extrapolation to larger and smaller masses.

The dashed lines represent the Tollet [123] result. In the halo mass range, $10^9 - 2 \times 10^{10} M_\odot$ of Fig. 1, the slope of our model flattens from -0.5 to values closer to zero, thus there is a maximum of core formation. In the SNF model [i.e. 135, the Macció model], core formation proceeds from significant alteration of the inner DM density profile from stellar feedback: the inner halo then expands, giving rise to a core. In the DFBC model (namely our model), the DF interaction between DM and baryons produces a "heating" of DM, with a consequent expansion, and the formation of a core.

In this mass range, Fig. 1 displays a similar trend to that of [123, 135].

Although the trends are similar, the slopes differ, especially below $10^{11} M_\odot$. In this range as well as in the other ranges, the difference in slope is due to the different ways the DFBC and SNF works. As discussed in the paper, for the DFBC, the flattening of density profiles is due to the "heating" of DM via interaction with baryons (gas clumps) through dynamical friction. Through this interaction, angular momentum and energy are exchanged between dark matter and clumps, resulting in the profile flattening. For the SNF, mass ejection from the supernovae leads to the same effect. A discriminating issue lies in the onset of the "heating" processes: the earlier those processes arise, the more efficiently they flatten the profile. The

⁶ The virial radius is defined as the radius at which the halo overdensity is $200 \rho_c$, being ρ_c the critical density

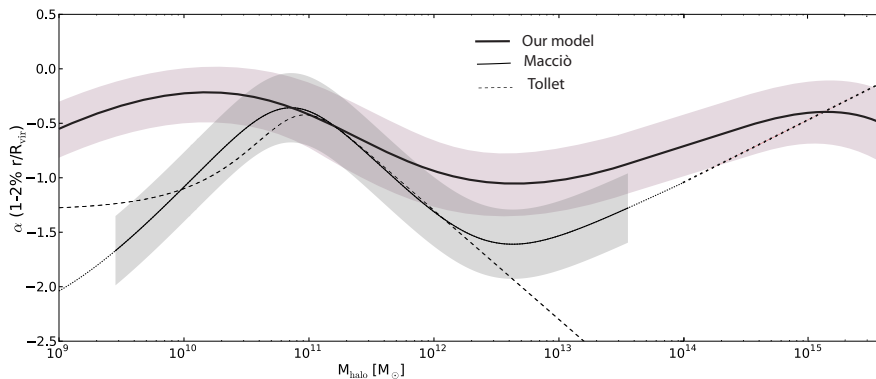


Figure 1. The inner slope-mass relation for the halo. The top thick line represents the result of this paper, the shaded region the $1\text{-}\sigma$ scatter. The bottom thin line represents the results of [135], and the shaded region the $1\text{-}\sigma$ scatter. The dashed line is the results of [123].

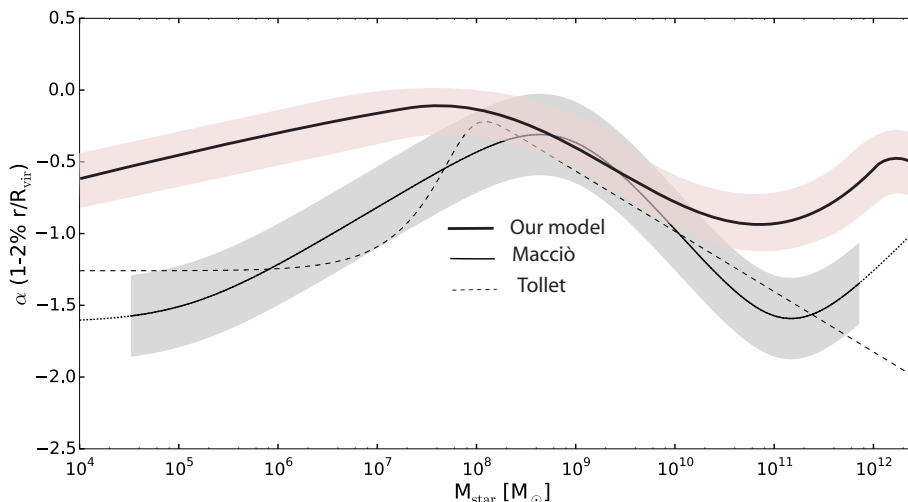


Figure 2. Inner slope-stellar mass relation. Symbols represent the same models as in Fig. 1.

series of steps SNF and DFBC require to flatten a profile are different. For the SNF, gas must form stars before these can explode as supernovae, if the mass is large enough. A longer and more complex series of events are needed to produce the observed density profile flattening than for the DFBC. To flatten the halo cusp and give rise to the core, the DFBC just requires the presence of gas clumps. Its flattening is therefore more ergonomic and efficient than the SNF model. As a result the process produces smaller slopes than through SNF.

After the maximum, both our result and that of Macciò steepen again, reaching values around -1 , in our model, and -1.6 for Macciò model, for masses of $4 \times 10^{12} M_{\odot}$.

That steepening, especially for the Macciò model based on SNF, is related to stars forming in the central regions, which deepens the gravitational potential, opposing SN feedback, and the DM expansion process. This produce a cuspier profile.

In the mass range above $4 \times 10^{12} M_{\odot}$, the slope starts to flatten.

In the case of the Macciò model, the flattening stops at the limit of their simulation, namely at 3.6×10^{13} . In our case, the flattening reaches a maximum at $\simeq 10^{15} M_{\odot}$, and is related to

the AGN feedback. This is similar to the flattening effect of SN feedback on smaller masses. Beyond the $\simeq 10^{15} M_{\odot}$ maximum, we observe again a steepening of the profile, because AGN feedback becomes less effective.

In Summary, while in [136], and [123], the behavior is non-monotonic with only one maximum of "core-formation", the behavior in our model is more complex, and presents two maxima of "core-formation". The first maximum is produced by the DFBC mechanism and SN feedback, while the second is produced by the DFBC mechanism and AGN feedback. The situation in the case of [135] is similar to that of [123] in the halo mass range $\simeq 2 \times 10^9 M_{\odot} - 10^{12} M_{\odot}$, where their slope flattens to a maximum at $\simeq 10^{11} M_{\odot}$. A relaxation of the halo is observed for masses larger than $\simeq 2 \times 10^{12} M_{\odot}$, as in the case of our model, with an inner slope flatter than the predictions of DM only N-body simulations.

At this point there are two important remarks. The first concerns an effect in the Macciò model that prevents it from producing shallow enough cores in the mass range $\simeq 10^{12} - 10^{13} M_{\odot}$: the number of stars forming in the central regions is so large that it can efficiently oppose the SN feedback. This produces a region with steeper slopes, with respect to the re-

$x [M_\odot]$	n	n_1	$x_0 [M_\odot]$	$x_1 [M_\odot]$	$x_2 [M_\odot]$	$x_3 [M_\odot]$
M_{halo}	-5.32	8.60	$1.50 \cdot 10^{25}$	$2.53 \cdot 10^{12}$	$3.52 \cdot 10^{-5}$	$2.49 \cdot 10^{10}$
M_\star	-0.46	3.94	$8.60 \cdot 10^{12}$	$9.34 \cdot 10^{10}$	$8.69 \cdot 10^2$	$1.27 \cdot 10^8$
	β	γ	δ	σ		$1-\sigma$
M_{halo}	1.14	0.26	0.43	1.15		0.32
M_\star	1.16	2.53	0.22	0.71		0.28

Table I. Parameters values for the fitting functions described in eqs. 13.

gion $\simeq 10^{11} - 10^{12} M_\odot$. This effect is not so important in the case of our model, and consequently we have shallower slopes. The second provides an extra reason for the slope difference in this region between our model and Macció's: the larger efficiency of the DFBC model compared with the SNF model, that does not need to wait for stars to form to start producing feedback on DM.

Our model and [135] have similar behavior until $\simeq 3.6 \times 10^{13} M_\odot$. As the Macció model [135] validity does not extend beyond $\simeq 3.6 \times 10^{13} M_\odot$, the comparison with our model cannot be extended to some of the masses it reaches.

The behavior of the inner slope α versus the stellar mass (Fig. (2)), M_\star is similar to that discussed for the case of M_{halo} : in our model, we observe the double maxima, as in the case of M_{halo} , at $M_\star \simeq 4 \times 10^7 M_\odot$, and $M_\star \simeq 10^{12} M_\odot$. For the [135] model, the situation of M_\star is similar to that of M_{halo} . In the [135] model, an up-turn for $M_\star > 10^{11} M_\odot$ is observed. The behavior of the inner slope as function of M_{halo} , or M_\star , can be represented by the functional forms

$$\alpha_{\star/\text{halo}}(x) = n - \log_{10} \left[n_1 \left(1 + \frac{x}{x_1} \right)^{-\beta} + \left(\frac{x}{x_0} \right)^\gamma \right] + \log_{10} \left[1 + \left(\frac{x}{x_2} \right)^\delta \right] - \log_{10} \left[1 + \left(\frac{x}{x_3} \right)^\sigma \right]. \quad (13)$$

Note the functional forms are identical but differ from the values of the functional break limit masses ($10^{14} M_\odot$ or $10^{12} M_\odot$), of the variables (M_{halo} or M_\star) and of the parameters, that are shown in Table I.

Figs. 1-2 also presents the scatter around both our and the [135] relations. These scatters are almost constant, and in the case of the slope-halo mass relation, the value of the average scatter is $\sigma \simeq 0.3$, while in the case of the slope-stellar mass relation it is $\sigma \simeq 0.27$. It was calculated using all the galaxies simulated. We do not plot all the galaxies so as to keep the figures legible.

Note that the slope behaviour, and by extension that of the DM density profile, for cluster-type masses can result from a model with two stages. The first dissipative phase sees the formation of the seed for the BCG, while the second, dissipationless stage is driven by the DF, between DM in the halo and the sunk baryonic clumps (to the centre), into flattening the density profile inner slope.

The large scatter of the inner slope among the cluster population reflects 1.) that the total mass density profile is given by the sum of the DM and baryon contents: $M_{\text{Total}} = M_{\text{BCG}} + M_{\text{DM}}$ 2.) haloes follow NFW-like density profiles 3.) the variations in the BCGs masses. This entails DM profile inner slopes ranges from the NFW slope to flatter slopes, depending on the amount of central baryons.

Before concluding, let us emphasize our results, in their differences with [123, 135]. The major difference lies in the larger range, from dwarf galaxies to clusters, described by our model, compared with [123, 135]. Indeed, Fig. (1) reveals that our model produces a flatter slope than [123, 135] in all mass ranges, except for a very small mass range close to $10^{11} M_\odot$. Our model's almost always shallower slope compared with [123, 135] stems from the more efficient flattening from the DFBC model, compared with the SNF model. This is particularly visible in the mass range $10^9 - 10^{10} M_\odot$. Close to $10^{11} M_\odot$, the energy released by supernovae is larger than the gravitational potential due to stars, resulting into a maximum efficiency of the SNF and a corresponding minimum (maximum flattening) for the [123, 135] slope, while our model outputs similar slopes. The intensity of the stars gravitational potential increases from $10^{11} M_\odot$ to $5 \times 10^{12} M_\odot$, consequently steepening the slope in the [123, 135] model. This behaviour occurs similarly in our model, due to the decrease in the exchange of energy between clumps and DM. It produces a shallower slope, reflecting the higher efficiency of the DFBC mechanism compared with the SNF, as pointed above. In the mass range $5 \times 10^{12} - 3.6 \times 10^{13} M_\odot$, AGN feedback starts to show its effect, in the [135] model and in ours, resulting in the observed flattening.

VI. CONCLUSIONS

Despite the facts that the Λ CDM model has shown many observational successes and that the Cusp/Core problem is better understood compared with a couple of decades ago, the Cusp/Core problem remains one of the prominent problems of the Λ CDM model. It consists in the discrepancy between the inner slope observed in dwarf galaxies, and the cuspy profiles obtained in N-body only simulations. One of its remaining issues concerns the understanding of the observed variations of inner slopes among different kinds of galaxies, as well as among galaxy clusters, with shallower than the standard Navarro-Frenk-White profiles. Following the mass dependence of galaxies inner slopes shown in [42], several SPH simulations studied the problem in detail.

Following the slope-mass relation obtained by [123, 136, 207] in the mass range covering dwarf galaxies up to Milky-Way sizes, and its extension by [135] to galaxy groups, this paper further extended the [135] results to the mass range of clusters of galaxies. For more massive structures than galaxies, the inner slope-mass relation continues to steepen until reaching a minimum and increasing again. Specifically, the slope-halo mass profile flattening starts at masses $\simeq 10^{12.4} M_\odot$ and reaches a maximum of core formation at $\simeq 10^{15} M_\odot$. This flattening is produced by the action of AGN

feedback, in a similar way to the role of SN feedback for smaller galaxy masses. Beyond this maximum of core formation, the trend reverts to steepening. The one-sigma scatter on α is approximately constant in the whole mass range ($\Delta\alpha \simeq 0.3$). Our slope-mass relation is a first step in determining a density profile taking into account baryons, for a larger mass range than for the profiles obtained by [207]. Indeed, the [207] density profile taking baryons into account is limited to the dwarf galaxies to Milky Way size mass range. We have extended this to clusters of galaxies. In a subsequent paper, we propose to find the density profile of structures, taking into account the role of baryons, in the mass range from dwarf galaxies to clusters. Despite well known

limitations in density profile inner slope determination, such model could then be compared with clusters mass extrapolation of the [135] results, also considering Milky Way dwarf spheroidals [87] and clusters from [22, 23].

ACKNOWLEDGMENTS

MLeD acknowledges the financial support by the Lanzhou University starting fund, the Fundamental Research Funds for the Central Universities (Grant No. Izujbky-2019-25), National Science Foundation of China (grant No. 12047501) and the 111 Project under Grant No. B20063. The authors wish to thank Maksym Deliyergiyev for some calculations.

-
- [1] Planck Collaboration, P. A. R. Ade, N. Aghanim, M. Arnaud, M. Ashdown, J. Aumont, C. Baccigalupi, A. J. Banday, R. B. Barreiro, J. G. Bartlett, and et al., *A&A* **594**, A13 (2016), [arXiv:1502.01589](#).
- [2] G. Bertone, D. Hooper, and J. Silk, *Physics Reports* **405**, 279 (2005), [arXiv:hep-ph/0404175](#).
- [3] A. Del Popolo, *International Journal of Modern Physics D* **23**, 1430005 (2014), [arXiv:1305.0456 \[astro-ph.CO\]](#).
- [4] A. G. Riess, A. V. Filippenko, P. Challis, and et al., *AJ* **116**, 1009 (1998), [arXiv:astro-ph/9805201](#).
- [5] S. Perlmutter, G. Aldering, G. Goldhaber, and et al., *ApJ* **517**, 565 (1999), [arXiv:astro-ph/9812133](#).
- [6] A. Del Popolo, *Astronomy Reports* **51**, 169 (2007), [arXiv:0801.1091](#).
- [7] E. Komatsu, K. M. Smith, J. Dunkley, and et al., *ApJS* **192**, 18 (2011), [arXiv:1001.4538 \[astro-ph.CO\]](#).
- [8] G. Hinshaw, D. Larson, E. Komatsu, D. N. Spergel, C. L. Bennett, J. Dunkley, M. R. Nolta, M. Halpern, R. S. Hill, and et al., *ApJS* **208**, 19 (2013), [arXiv:1212.5226 \[astro-ph.CO\]](#).
- [9] A. Del Popolo, in *AIP Conf. Proc.*, Vol. 1548 (2013) pp. 2–63.
- [10] Planck Collaboration, P. A. R. Ade, N. Aghanim, C. Armitage-Caplan, M. Arnaud, M. Ashdown, F. Atrio-Barandela, J. Aumont, C. Baccigalupi, A. J. Banday, and et al., *A&A* **571**, A16 (2014), [arXiv:1303.5076](#).
- [11] S. Weinberg, *Reviews of Modern Physics* **61**, 1 (1989).
- [12] A. V. Astashenok and A. del Popolo, *Classical and Quantum Gravity* **29**, 085014 (2012), [arXiv:1203.2290 \[gr-qc\]](#).
- [13] A. Del Popolo, F. Pace, and J. A. S. Lima, *International Journal of Modern Physics D* **22**, 1350038 (2013), [arXiv:1207.5789 \[astro-ph.CO\]](#).
- [14] A. Del Popolo, F. Pace, and J. A. S. Lima, *MNRAS* **430**, 628 (2013), [arXiv:1212.5092 \[astro-ph.CO\]](#).
- [15] A. Del Popolo, F. Pace, S. P. Maydanyuk, J. A. S. Lima, and J. F. Jesus, *Phys. Rev. D* **87**, 043527 (2013), [arXiv:1303.3628 \[astro-ph.CO\]](#).
- [16] K. Bolejko, *Phys. Rev. D* **97**, 103529 (2018), [arXiv:1712.02967 \[astro-ph.CO\]](#).
- [17] M. Raveri, *Phys. Rev. D* **93**, 043522 (2016).
- [18] E. Macaulay, I. K. Wehus, and H. K. Eriksen, *Physical Review Letters* **111**, 161301 (2013), [arXiv:1303.6583](#).
- [19] A. Del Popolo and M. Gambera, *A&A* **357**, 809 (2000), [astro-ph/9909156](#).
- [20] A. Del Popolo, *MNRAS* **336**, 81 (2002), [astro-ph/0205449](#).
- [21] A. Del Popolo and V. F. Cardone, *MNRAS* **423**, 1060 (2012), [arXiv:1203.3377 \[astro-ph.CO\]](#).
- [22] A. B. Newman, T. Treu, R. S. Ellis, D. J. Sand, C. Nipoti, J. Richard, and E. Jullo, *ApJ* **765**, 24 (2013), [arXiv:1209.1391 \[astro-ph.CO\]](#).
- [23] A. B. Newman, T. Treu, R. S. Ellis, and D. J. Sand, *ApJ* **765**, 25 (2013), [arXiv:1209.1392 \[astro-ph.CO\]](#).
- [24] A. Del Popolo, F. Pace, and M. Le Delliou, *JCAP* **3**, 032 (2017), [arXiv:1703.06918](#).
- [25] A. Del Popolo, F. Pace, M. Le Delliou, and X. Lee, *Phys. Rev. D* **98**, 063517 (2018), [arXiv:1809.10609 \[astro-ph.GA\]](#).
- [26] B. Moore, T. Quinn, F. Governato, J. Stadel, and G. Lake, *MNRAS* **310**, 1147 (1999), [astro-ph/9903164](#).
- [27] M. Boylan-Kolchin, J. S. Bullock, and M. Kaplinghat, *MNRAS* **415**, L40 (2011), [arXiv:1103.0007 \[astro-ph.CO\]](#).
- [28] M. Boylan-Kolchin, J. S. Bullock, and M. Kaplinghat, *MNRAS* **422**, 1203 (2012), [arXiv:1111.2048 \[astro-ph.CO\]](#).
- [29] A. Zolotov, A. M. Brooks, B. Willman, F. Governato, A. Pontzen, C. Christensen, A. Dekel, T. Quinn, S. Shen, and J. Wadsley, *ApJ* **761**, 71 (2012), [arXiv:1207.0007 \[astro-ph.CO\]](#).
- [30] A. Del Popolo, J. A. S. Lima, J. C. Fabris, and D. C. Rodrigues, *JCAP* **4**, 021 (2014), [arXiv:1404.3674](#).
- [31] B. Moore, *Nature (London)* **370**, 629 (1994).
- [32] R. A. Flores and J. R. Primack, *ApJL* **427**, L1 (1994), [astro-ph/9402004](#).
- [33] J. F. Navarro, C. S. Frenk, and S. D. M. White, *ApJ* **462**, 563 (1996), [astro-ph/9508025](#).
- [34] J. F. Navarro, C. S. Frenk, and S. D. M. White, *ApJ* **490**, 493 (1997), [astro-ph/9611107](#).
- [35] J. F. Navarro, A. Ludlow, V. Springel, J. Wang, M. Vogelsberger, S. D. M. White, A. Jenkins, C. S. Frenk, and A. Helmi, *MNRAS* **402**, 21 (2010), [arXiv:0810.1522](#).
- [36] B. Moore, F. Governato, T. Quinn, J. Stadel, and G. Lake, *ApJL* **499**, L5+ (1998), [astro-ph/9709051](#).
- [37] T. Fukushige and J. Makino, *ApJ* **557**, 533 (2001), [astro-ph/0008104](#).
- [38] Y. P. Jing and Y. Suto, *ApJL* **529**, L69 (2000), [astro-ph/9909478](#).
- [39] M. Ricotti, *MNRAS* **344**, 1237 (2003), [astro-ph/0212146](#).
- [40] M. Ricotti and M. I. Wilkinson, *MNRAS* **353**, 867 (2004), [astro-ph/0406297](#).
- [41] M. Ricotti, A. Pontzen, and M. Viel, *ApJL* **663**, L53 (2007), [arXiv:0706.0856](#).

- [42] A. Del Popolo, *MNRAS* **408**, 1808 (2010), arXiv:1012.4322 [astro-ph.CO].
- [43] V. F. Cardone, A. Del Popolo, C. Tortora, and N. R. Napolitano, *MNRAS* **416**, 1822 (2011), arXiv:1106.0364 [astro-ph.CO].
- [44] A. Del Popolo, *JCAP* **7**, 014 (2011), arXiv:1112.4185 [astro-ph.CO].
- [45] A. Del Popolo, V. F. Cardone, and G. Belvedere, *MNRAS* **429**, 1080 (2013), arXiv:1212.6797 [astro-ph.CO].
- [46] A. Di Cintio, C. B. Brook, A. A. Dutton, A. V. Macciò, G. S. Stinson, and A. Knebe, *Mon. Not. Roy. Astron. Soc.* **441**, 2986 (2014), arXiv:1404.5959 [astro-ph.CO].
- [47] J. Stadel, D. Potter, B. Moore, J. Diemand, P. Madau, M. Zemp, M. Kuhlen, and V. Quilis, *MNRAS* **398**, L21 (2009), arXiv:0808.2981.
- [48] L. Gao, J. F. Navarro, S. Cole, C. S. Frenk, S. D. M. White, V. Springel, A. Jenkins, and A. F. Neto, *MNRAS* **387**, 536 (2008), arXiv:0711.0746.
- [49] E. Polisensky and M. Ricotti, *MNRAS* **450**, 2172 (2015), arXiv:1504.02126.
- [50] F. Governato, C. Brook, L. Mayer, A. Brooks, G. Rhee, J. Wadsley, P. Jonsson, B. Willman, G. Stinson, T. Quinn, and P. Madau, *Nature (London)* **463**, 203 (2010), arXiv:0911.2237 [astro-ph.CO].
- [51] F. Governato, A. Zolotov, A. Pontzen, C. Christensen, S. H. Oh, A. M. Brooks, T. Quinn, S. Shen, and J. Wadsley, *MNRAS* **422**, 1231 (2012), arXiv:1202.0554 [astro-ph.CO].
- [52] A. Del Popolo, *ApJ* **698**, 2093 (2009), arXiv:0906.4447 [astro-ph.CO].
- [53] V. F. Cardone and A. Del Popolo, *MNRAS* **427**, 3176 (2012), arXiv:1209.1524 [astro-ph.CO].
- [54] A. Del Popolo, *MNRAS* **419**, 971 (2012), arXiv:1105.0090 [astro-ph.CO].
- [55] A. Del Popolo, *MNRAS* **424**, 38 (2012), arXiv:1204.4439 [astro-ph.CO].
- [56] A. Del Popolo and N. Hiotelis, *JCAP* **1**, 047 (2014), arXiv:1401.6577 [astro-ph.GA].
- [57] A. Burkert, *ApJL* **447**, L25 (1995), astro-ph/9504041.
- [58] W. J. G. de Blok, A. Bosma, and S. McGaugh, *MNRAS* **340**, 657 (2003), astro-ph/0212102.
- [59] R. A. Swaters, B. F. Madore, F. C. van den Bosch, and M. Balcells, *ApJ* **583**, 732 (2003), astro-ph/0210152.
- [60] R. Kuzio de Naray and T. Kaufmann, *MNRAS* **414**, 3617 (2011), arXiv:1012.3471 [astro-ph.CO].
- [61] S.-H. Oh, W. J. G. de Blok, E. Brinks, F. Walter, and R. C. Kennicutt, Jr., *AJ* **141**, 193 (2011), arXiv:1011.0899 [astro-ph.CO].
- [62] S.-H. Oh, C. Brook, F. Governato, E. Brinks, L. Mayer, W. J. G. de Blok, A. Brooks, and F. Walter, *AJ* **142**, 24 (2011), arXiv:1011.2777 [astro-ph.CO].
- [63] D. J. Sand, T. Treu, and R. S. Ellis, *ApJL* **574**, L129 (2002), astro-ph/0207048.
- [64] D. J. Sand, T. Treu, G. P. Smith, and R. S. Ellis, *ApJ* **604**, 88 (2004), astro-ph/0309465.
- [65] A. Del Popolo, M. Le Delliou, and X. Lee, *Phys. Dark Univ.* **26**, 100342 (2019).
- [66] W. J. G. de Blok and S. S. McGaugh, *MNRAS* **290**, 533 (1997), astro-ph/9704274.
- [67] M. Spano, M. Marcellin, P. Amram, C. Carignan, B. Epinat, and O. Hernandez, *MNRAS* **383**, 297 (2008), arXiv:0710.1345.
- [68] J. D. Simon, A. D. Bolatto, A. Leroy, L. Blitz, and E. L. Gates, *ApJ* **621**, 757 (2005), astro-ph/0412035.
- [69] W. J. G. de Blok, F. Walter, E. Brinks, C. Trachternach, S.-H. Oh, and R. C. Kennicutt, Jr., *AJ* **136**, 2648 (2008), arXiv:0810.2100.
- [70] T. P. K. Martinsson, M. A. W. Verheijen, K. B. Westfall, M. A. Bershad, D. R. Andersen, and R. A. Swaters, *A&A* **557**, A131 (2013), arXiv:1308.0336 [astro-ph.CO].
- [71] J. D. Simon, A. D. Bolatto, A. Leroy, and L. Blitz, *ApJ* **596**, 957 (2003), astro-ph/0307154.
- [72] J. J. Adams, K. Gebhardt, G. A. Blanc, M. H. Fabricius, G. J. Hill, J. D. Murphy, R. C. E. van den Bosch, and G. van de Ven, *ApJ* **745**, 92 (2012), arXiv:1110.5951 [astro-ph.CO].
- [73] J. J. Adams, J. D. Simon, M. H. Fabricius, R. C. E. van den Bosch, J. C. Barentine, R. Bender, K. Gebhardt, G. J. Hill, J. D. Murphy, R. A. Swaters, J. Thomas, and G. van de Ven, *ApJ* **789**, 63 (2014), arXiv:1405.4854.
- [74] G. Battaglia, A. Helmi, and M. Breddels, *New Astronomy Reviews* **57**, 52 (2013), arXiv:1305.5965 [astro-ph.CO].
- [75] N. W. Evans, J. An, and M. G. Walker, *MNRAS* **393**, L50 (2009), arXiv:0811.1488.
- [76] J. Wolf and J. S. Bullock, ArXiv e-prints, 1203.4240 (2012), arXiv:1203.4240 [astro-ph.CO].
- [77] K. Hayashi and M. Chiba, *ApJ* **755**, 145 (2012), arXiv:1206.3888 [astro-ph.CO].
- [78] T. Richardson and M. Fairbairn, *MNRAS* **432**, 3361 (2013), arXiv:1207.1709 [astro-ph.CO].
- [79] J. R. Jardel and K. Gebhardt, *ApJ* **746**, 89 (2012), arXiv:1112.0319 [astro-ph.CO].
- [80] M. A. Breddels, A. Helmi, R. C. E. van den Bosch, G. van de Ven, and G. Battaglia, *MNRAS* **433**, 3173 (2013), arXiv:1205.4712 [astro-ph.CO].
- [81] J. R. Jardel and K. Gebhardt, *ApJL* **775**, L30 (2013).
- [82] J. R. Jardel, K. Gebhardt, M. H. Fabricius, N. Drory, and M. J. Williams, *ApJ* **763**, 91 (2013), arXiv:1211.5376 [astro-ph.CO].
- [83] G. Battaglia, A. Helmi, E. Tolstoy, M. Irwin, V. Hill, and P. Jablonka, *ApJL* **681**, L13 (2008), arXiv:0802.4220.
- [84] M. G. Walker and J. Peñarrubia, *ApJ* **742**, 20 (2011), arXiv:1108.2404.
- [85] A. Agnello and N. W. Evans, *ApJL* **754**, L39 (2012), arXiv:1205.6673 [astro-ph.GA].
- [86] N. C. Amorisco and N. W. Evans, *MNRAS* **419**, 184 (2012), arXiv:1106.1062 [astro-ph.CO].
- [87] K. Hayashi, M. Chiba, and T. Ishiyama, *Astrophys. J.* **904**, 45 (2020), arXiv:2007.13780 [astro-ph.GA].
- [88] S. Shao, M. Cautun, C. S. Frenk, M. Reina-Campos, A. J. Deason, R. A. Crain, J. D. Kruijssen, and J. Pfeffer, (2020), arXiv:2012.08058 [astro-ph.GA].
- [89] A. R. Zentner and J. S. Bullock, *ApJ* **598**, 49 (2003), astro-ph/0304292.
- [90] P. Colín, V. Avila-Reese, and O. Valenzuela, *ApJ* **542**, 622 (2000), astro-ph/0004115.
- [91] J. Goodman, *New Astronomy* **5**, 103 (2000), astro-ph/0003018.
- [92] W. Hu, R. Barkana, and A. Gruzinov, *Physical Review Letters* **85**, 1158 (2000), astro-ph/0003365.
- [93] M. Kaplinghat, L. Knox, and M. S. Turner, *Physical Review Letters* **85**, 3335 (2000), astro-ph/0005210.
- [94] P. J. E. Peebles, *ApJL* **534**, L127 (2000), astro-ph/0002495.
- [95] J. Sommer-Larsen and A. Dolgov, *ApJ* **551**, 608 (2001), astro-ph/9912166.
- [96] H. A. Buchdahl, *MNRAS* **150**, 1 (1970).
- [97] A. A. Starobinsky, *Physics Letters B* **91**, 99 (1980).
- [98] G. R. Bengochea and R. Ferraro, *Phys. Rev. D* **79**, 124019 (2009), arXiv:0812.1205.

- [99] E. V. Linder, *Phys. Rev. D* **81**, 127301 (2010), [arXiv:1005.3039](#) [[astro-ph.CO](#)].
- [100] J. B. Dent, S. Dutta, and E. N. Saridakis, *JCAP* **1**, 9 (2011), [arXiv:1010.2215](#) [[astro-ph.CO](#)].
- [101] R. Zheng and Q.-G. Huang, *JCAP* **3**, 2 (2011), [arXiv:1010.3512](#) [[gr-qc](#)].
- [102] M. Milgrom, *ApJ* **270**, 371 (1983).
- [103] M. Milgrom, *ApJ* **270**, 365 (1983).
- [104] J. F. Navarro, V. R. Eke, and C. S. Frenk, *MNRAS* **283**, L72 (1996), [astro-ph/9610187](#).
- [105] S. Gelato and J. Sommer-Larsen, *MNRAS* **303**, 321 (1999), [astro-ph/9806289](#).
- [106] J. I. Read and G. Gilmore, *MNRAS* **356**, 107 (2005), [astro-ph/0409565](#).
- [107] S. Mashchenko, H. M. P. Couchman, and A. Sills, *ApJ* **639**, 633 (2006), [astro-ph/0511361](#).
- [108] S. Mashchenko, J. Wadsley, and H. M. P. Couchman, *Science* **319**, 174 (2008), [arXiv:0711.4803](#).
- [109] J. Oñorbe, M. Boylan-Kolchin, J. S. Bullock, P. F. Hopkins, D. Kerès, C.-A. Faucher-Giguère, E. Quataert, and N. Murray, *Mon. Not. Roy. Astron. Soc.* **454**, 2092 (2015), [arXiv:1502.02036](#) [[astro-ph.GA](#)].
- [110] K. El-Badry, A. R. Wetzel, M. Geha, E. Quataert, P. F. Hopkins, D. Kereš, T. K. Chan, and C.-A. Faucher-Giguère, *ApJ* **835**, 193 (2017), [arXiv:1610.04232](#) [[astro-ph.GA](#)].
- [111] A. Fitts *et al.*, *Mon. Not. Roy. Astron. Soc.* **471**, 3547 (2017), [arXiv:1611.02281](#) [[astro-ph.GA](#)].
- [112] A. El-Zant, I. Shlosman, and Y. Hoffman, *ApJ* **560**, 636 (2001), [astro-ph/0103386](#).
- [113] A. A. El-Zant, Y. Hoffman, J. Primack, F. Combes, and I. Shlosman, *ApJL* **607**, L75 (2004), [astro-ph/0309412](#).
- [114] C.-P. Ma and M. Boylan-Kolchin, *Physical Review Letters* **93**, 021301 (2004), [astro-ph/0403102](#).
- [115] C. Nipoti, T. Treu, L. Ciotti, and M. Stiavelli, *MNRAS* **355**, 1119 (2004), [astro-ph/0404127](#).
- [116] E. Romano-Díaz, I. Shlosman, Y. Hoffman, and C. Heller, *ApJL* **685**, L105 (2008), [arXiv:0808.0195](#).
- [117] E. Romano-Díaz, I. Shlosman, C. Heller, and Y. Hoffman, *ApJ* **702**, 1250 (2009), [arXiv:0901.1317](#) [[astro-ph.CO](#)].
- [118] D. R. Cole, W. Dehnen, and M. I. Wilkinson, *MNRAS* **416**, 1118 (2011), [arXiv:1105.4050](#) [[astro-ph.CO](#)].
- [119] S. Inoue and T. R. Saitoh, *MNRAS* **418**, 2527 (2011), [arXiv:1108.0906](#) [[astro-ph.CO](#)].
- [120] C. Nipoti and J. Binney, *MNRAS* **446**, 1820 (2015), [arXiv:1410.6169](#).
- [121] R. Teyssier, A. Pontzen, Y. Dubois, and J. I. Read, *MNRAS* **429**, 3068 (2013), [arXiv:1206.4895](#) [[astro-ph.CO](#)].
- [122] T. Chan, D. Kereš, J. Oñorbe, P. Hopkins, A. Muratov, C. A. Faucher-Giguère, and E. Quataert, *Mon. Not. Roy. Astron. Soc.* **454**, 2981 (2015), [arXiv:1507.02282](#) [[astro-ph.GA](#)].
- [123] E. Tollet *et al.*, *Mon. Not. Roy. Astron. Soc.* **456**, 3542 (2016), [Erratum: *Mon. Not. Roy. Astron. Soc.* **487**, 1764 (2019)], [arXiv:1507.03590](#) [[astro-ph.GA](#)].
- [124] S. Bose *et al.*, *Mon. Not. Roy. Astron. Soc.* **486**, 4790 (2019), [arXiv:1810.03635](#) [[astro-ph.GA](#)].
- [125] F. Walter, E. Brinks, W. J. G. de Blok, F. Bigiel, R. C. Kennicutt, Jr., M. D. Thornley, and A. Leroy, *AJ* **136**, 2563 (2008), [arXiv:0810.2125](#).
- [126] S.-H. Oh, W. J. G. de Blok, F. Walter, E. Brinks, and R. C. Kennicutt, Jr., *AJ* **136**, 2761 (2008), [arXiv:0810.2119](#).
- [127] S. Trujillo-Gomez, A. Klypin, P. Colín, D. Ceverino, K. S. Arraki, and J. Primack, *MNRAS* **446**, 1140 (2015), [arXiv:1311.2910](#).
- [128] I. Ferrero, M. G. Abadi, J. F. Navarro, L. V. Sales, and S. Gurovich, *MNRAS* **425**, 2817 (2012), [arXiv:1111.6609](#) [[astro-ph.CO](#)].
- [129] J. Peñarrubia, A. Pontzen, M. G. Walker, and S. E. Koposov, *ApJL* **759**, L42 (2012), [arXiv:1207.2772](#) [[astro-ph.GA](#)].
- [130] S. Garrison-Kimmel, M. Rocha, M. Boylan-Kolchin, J. S. Bullock, and J. Lally, *MNRAS* **433**, 3539 (2013), [arXiv:1301.3137](#) [[astro-ph.CO](#)].
- [131] S. Garrison-Kimmel, M. Boylan-Kolchin, J. S. Bullock, and E. N. Kirby, *MNRAS* **444**, 222 (2014), [arXiv:1404.5313](#).
- [132] E. Papastergis, R. Giovanelli, M. P. Haynes, and F. Shankar, *A&A* **574**, A113 (2015), [arXiv:1407.4665](#).
- [133] J. Oñorbe, M. Boylan-Kolchin, J. S. Bullock, P. F. Hopkins, D. Kerès, C.-A. Faucher-Giguère, E. Quataert, and N. Murray, *ArXiv e-prints* (2015), [arXiv:1502.02036](#).
- [134] H. Katz, F. Lelli, S. S. McGaugh, A. Di Cintio, C. B. Brook, and J. M. Schombert, *Mon. Not. Roy. Astron. Soc.* **466**, 1648 (2017), [arXiv:1605.05971](#) [[astro-ph.GA](#)].
- [135] A. V. Macciò, S. Crespi, M. Blank, and X. Kang, *Mon. Not. Roy. Astron. Soc.* **495**, L46 (2020), [arXiv:2004.03817](#) [[astro-ph.GA](#)].
- [136] A. Del Popolo and F. Pace, *Astrophysics and Space Science* **361**, 162 (2016), [arXiv:1502.01947](#).
- [137] A. Del Popolo and P. Kroupa, *A&A* **502**, 733 (2009), [arXiv:0906.1146](#) [[astro-ph.CO](#)].
- [138] D. Martizzi, R. Teyssier, B. Moore, and T. Wentz, *MNRAS* **422**, 3081 (2012), [arXiv:1112.2752](#) [[astro-ph.CO](#)].
- [139] A. Del Popolo and M. Gambera, *A&A* **308**, 373 (1996).
- [140] A. Del Popolo, *JCAP* **7**, 019 (2014), [arXiv:1407.4347](#).
- [141] A. Lazar *et al.*, *Mon. Not. Roy. Astron. Soc.* **497**, 2393 (2020), [arXiv:2004.10817](#) [[astro-ph.GA](#)].
- [142] J. E. Gunn and J. R. Gott, III, *ApJ* **176**, 1 (1972).
- [143] E. Bertschinger, *ApJS* **58**, 39 (1985).
- [144] Y. Hoffman and J. Shaham, *ApJ* **297**, 16 (1985).
- [145] B. S. Ryden and J. E. Gunn, *ApJ* **318**, 15 (1987).
- [146] Y. Ascasibar, G. Yepes, S. Gottlöber, and V. Müller, *MNRAS* **352**, 1109 (2004), [arXiv:astro-ph/0312221](#).
- [147] L. L. R. Williams, A. Babul, and J. J. Dalcanton, *ApJ* **604**, 18 (2004), [astro-ph/0312002](#).
- [148] B. S. Ryden, *ApJ* **329**, 589 (1988).
- [149] A. Del Popolo and M. Gambera, *A&A* **321**, 691 (1997), [astro-ph/9610052](#).
- [150] G. R. Blumenthal, S. M. Faber, R. Flores, and J. R. Primack, *ApJ* **301**, 27 (1986).
- [151] O. Y. Gnedin, A. V. Kravtsov, A. A. Klypin, and D. Nagai, *ApJ* **616**, 16 (2004), [astro-ph/0406247](#).
- [152] A. Klypin, H. Zhao, and R. S. Somerville, *ApJ* **573**, 597 (2002), [astro-ph/0110390](#).
- [153] M. Gustafsson, M. Fairbairn, and J. Sommer-Larsen, *Phys. Rev. D* **74**, 123522 (2006), [astro-ph/0608634](#).
- [154] G. De Lucia and A. Helmi, *MNRAS* **391**, 14 (2008), [arXiv:0804.2465](#).
- [155] Y.-S. Li, G. De Lucia, and A. Helmi, *MNRAS* **401**, 2036 (2010), [arXiv:0909.1291](#) [[astro-ph.GA](#)].
- [156] A. Del Popolo, *Astrophysics and Space Science* **361**, 222 (2016), [arXiv:1607.07408](#).
- [157] A. Del Popolo, *Astrophys. Space Sci.* **361**, 222 (2016), [arXiv:1607.07408](#) [[astro-ph.GA](#)].
- [158] A. Pontzen and F. Governato, *MNRAS* **421**, 3464 (2012), [arXiv:1106.0499](#) [[astro-ph.CO](#)].
- [159] J. E. Gunn, *ApJ* **218**, 592 (1977).
- [160] J. A. Fillmore and P. Goldreich, *ApJ* **281**, 1 (1984).
- [161] E. Komatsu, J. Dunkley, M. R. Nolta, and et al., *ApJS* **180**, 330 (2009), [arXiv:0803.0547](#).

- [162] F. Hoyle, *ApJ* **118**, 513 (1953).
- [163] P. J. E. Peebles, *ApJ* **155**, 393 (1969).
- [164] S. D. M. White, *ApJ* **286**, 38 (1984).
- [165] D. J. Eisenstein and A. Loeb, *ApJ* **439**, 520 (1995), [arXiv:astro-ph/9405012](#).
- [166] V. Avila-Reese, C. Firmani, and X. Hernández, *ApJ* **505**, 37 (1998), [astro-ph/9710201](#).
- [167] A. Toomre, *ApJ* **139**, 1217 (1964).
- [168] J. Binney and S. Tremaine, *Second Edition, 2008, Princeton, NJ, Princeton University Press, 1987, 747 p.* (1987).
- [169] M. R. Krumholz and A. Dekel, *MNRAS* **406**, 112 (2010), [arXiv:1001.0765](#).
- [170] A. Dekel, R. Sari, and D. Ceverino, *ApJ* **703**, 785 (2009), [arXiv:0901.2458 \[astro-ph.GA\]](#).
- [171] D. Ceverino, A. Dekel, N. Mandelker, F. Bournaud, A. Burkert, R. Genzel, and J. Primack, *MNRAS* **420**, 3490 (2012), [arXiv:1106.5587](#).
- [172] A. Del Popolo and M. Le Delliou, *JCAP* **12**, 051 (2014), [arXiv:1408.4893](#).
- [173] D. Ceverino, A. Dekel, and F. Bournaud, *MNRAS* **404**, 2151 (2010), [arXiv:0907.3271 \[astro-ph.CO\]](#).
- [174] J. Perez, O. Valenzuela, P. B. Tissera, and L. Michel-Dansac, *MNRAS* **436**, 259 (2013), [arXiv:1308.4396](#).
- [175] V. Perret, F. Renaud, B. Epinat, P. Amram, F. Bournaud, T. Contini, R. Teyssier, and J. C. Lambert, *Astron. Astrophys.* **562**, A1 (2014), [arXiv:1307.7130 \[astro-ph.CO\]](#).
- [176] D. Ceverino, A. Klypin, E. Klimek, S. Trujillo-Gomez, C. W. Churchill, and J. Primack, *Mon. Not. Roy. Astron. Soc.* **442**, 1545 (2014), [arXiv:1307.0943 \[astro-ph.CO\]](#).
- [177] D. Ceverino, A. Dekel, D. Tweed, and J. Primack, *Mon. Not. Roy. Astron. Soc.* **447**, 3291 (2015), [arXiv:1409.2622 \[astro-ph.GA\]](#).
- [178] F. Bournaud, V. Perret, F. Renaud, A. Dekel, B. G. Elmegreen, D. M. Elmegreen, R. Teyssier, P. Amram, E. Daddi, P.-A. Duc, D. Elbaz, B. Epinat, J. M. Gabor, S. Juneau, K. Kraljic, and E. Le Floch, *ApJ* **780**, 57 (2014), [arXiv:1307.7136 \[astro-ph.CO\]](#).
- [179] M. Behrendt, A. Burkert, and M. Schartmann, *ApJL* **819**, L2 (2016), [arXiv:1512.03430](#).
- [180] D. M. Elmegreen, B. G. Elmegreen, and A. C. Hirst, *ApJL* **604**, L21 (2004), [astro-ph/0402477](#).
- [181] D. M. Elmegreen, B. G. Elmegreen, M. T. Marcus, K. Shahinyan, A. Yau, and M. Petersen, *ApJ* **701**, 306 (2009), [arXiv:0906.2660 \[astro-ph.CO\]](#).
- [182] R. Genzel, S. Newman, T. Jones, N. M. Förster Schreiber, K. Shapiro, S. Genel, S. J. Lilly, and et al., *ApJ* **733**, 101 (2011), [arXiv:1011.5360 \[astro-ph.CO\]](#).
- [183] Y. Guo, M. Giavalisco, H. C. Ferguson, P. Cassata, and A. M. Koekemoer, *ApJ* **757**, 120 (2012), [arXiv:1110.3800](#).
- [184] S. Wuyts, N. M. Förster Schreiber, E. J. Nelson, P. G. van Dokkum, G. Brammer, Y.-Y. Chang, S. M. Faber, H. C. Ferguson, M. Franx, M. Fumagalli, R. Genzel, N. A. Grogan, D. D. Kocevski, A. M. Koekemoer, B. Lundgren, D. Lutz, E. J. McGrath, I. Momcheva, D. Rosario, R. E. Skelton, L. J. Tacconi, A. van der Wel, and K. E. Whitaker, *ApJ* **779**, 135 (2013), [arXiv:1310.5702](#).
- [185] Y. Guo, H. C. Ferguson, E. F. Bell, D. C. Koo, C. J. Conselice, M. Giavalisco, S. Kassin, Y. Lu, R. Lucas, N. Mandelker, D. M. McIntosh, J. R. Primack, S. Ravindranath, G. Barro, D. Ceverino, A. Dekel, S. M. Faber, J. J. Fang, A. M. Koekemoer, K. Noeske, M. Rafelski, and A. Straughn, *ApJ* **800**, 39 (2015), [arXiv:1410.7398](#).
- [186] D. M. Elmegreen, B. G. Elmegreen, S. Ravindranath, and D. A. Coe, *ApJ* **658**, 763 (2007), [astro-ph/0701121](#).
- [187] M. Noguchi, *Nature (London)* **392**, 253 (1998).
- [188] M. Noguchi, *ApJ* **514**, 77 (1999), [astro-ph/9806355](#).
- [189] M. Aumer, A. Burkert, P. H. Johansson, and R. Genzel, *ApJ* **719**, 1230 (2010), [arXiv:1007.0169](#).
- [190] H. Baumgardt and P. Kroupa, *MNRAS* **380**, 1589 (2007), [arXiv:0707.1944](#).
- [191] M. R. Krumholz and J. C. Tan, *ApJ* **654**, 304 (2007).
- [192] B. G. Elmegreen, F. Bournaud, and D. M. Elmegreen, *ApJ* **688**, 67 (2008), [arXiv:0808.0716](#).
- [193] B. G. Elmegreen, D. M. Elmegreen, J. Sánchez Almeida, C. Muñoz-Tuñón, J. Dewberry, J. Putko, Y. Teich, and M. Popinchalk, *ApJ* **774**, 86 (2013), [arXiv:1308.0306](#).
- [194] C. A. Garland, D. J. Pisano, M.-M. Mac Low, K. Kreckel, K. Rabidoux, and R. Guzmán, *ApJ* **807**, 134 (2015), [arXiv:1506.04649](#).
- [195] N. Mandelker, A. Dekel, D. Ceverino, C. DeGraf, Y. Guo, and J. Primack, *Mon. Not. Roy. Astron. Soc.* **464**, 635 (2017), [arXiv:1512.08791 \[astro-ph.GA\]](#).
- [196] A. V. Kravtsov, O. Y. Gnedin, and A. A. Klypin, *ApJ* **609**, 482 (2004), [astro-ph/0401088](#).
- [197] S. D. M. White and C. S. Frenk, *ApJ* **379**, 52 (1991).
- [198] D. J. Croton, V. Springel, S. D. M. White, G. De Lucia, C. S. Frenk, L. Gao, A. Jenkins, G. Kauffmann, J. F. Navarro, and N. Yoshida, *MNRAS* **365**, 11 (2006), [astro-ph/0508046](#).
- [199] G. Chabrier, *PASP* **115**, 763 (2003), [astro-ph/0304382](#).
- [200] D. Martizzi, R. Teyssier, and B. Moore, *MNRAS* **420**, 2859 (2012), [arXiv:1106.5371 \[astro-ph.CO\]](#).
- [201] C. M. Booth and J. Schaye, *Monthly Notices of the Royal Astronomical Society* **398**, 53 (2009).
- [202] A. Cattaneo, A. Dekel, J. Devriendt, B. Guiderdoni, and J. Blaizot, *MNRAS* **370**, 1651 (2006), [astro-ph/0601295](#).
- [203] D. Martizzi, R. Teyssier, and B. Moore, *MNRAS* **432**, 1947 (2013), [arXiv:1211.2648](#).
- [204] A. A. Klypin, S. Trujillo-Gomez, and J. Primack, *ApJ* **740**, 102 (2011), [arXiv:1002.3660](#).
- [205] A. J. Benson, *New Astronomy* **17**, 175 (2012), [arXiv:1008.1786](#).
- [206] O. Y. Gnedin and H. Zhao, *MNRAS* **333**, 299 (2002), [astro-ph/0108108](#).
- [207] A. Di Cintio, C. B. Brook, A. A. Dutton, A. V. Macciò, G. S. Stinson, and A. Knebe, *Mon. Not. Roy. Astron. Soc.* **441**, 2986 (2014), [arXiv:1404.5959 \[astro-ph.CO\]](#).